

Technical University of Denmark



The axial dipole moment of two intersecting spheres of equal radii

McAllister, Iain Wilson

Published in:
Journal of Applied Physics

Link to article, DOI:
[10.1063/1.341075](https://doi.org/10.1063/1.341075)

Publication date:
1988

Document Version
Publisher's PDF, also known as Version of record

[Link back to DTU Orbit](#)

Citation (APA):
McAllister, I. W. (1988). The axial dipole moment of two intersecting spheres of equal radii. Journal of Applied Physics, 63(6), 2158-2160. DOI: 10.1063/1.341075

DTU Library

Technical Information Center of Denmark

General rights

Copyright and moral rights for the publications made accessible in the public portal are retained by the authors and/or other copyright owners and it is a condition of accessing publications that users recognise and abide by the legal requirements associated with these rights.

- Users may download and print one copy of any publication from the public portal for the purpose of private study or research.
- You may not further distribute the material or use it for any profit-making activity or commercial gain
- You may freely distribute the URL identifying the publication in the public portal

If you believe that this document breaches copyright please contact us providing details, and we will remove access to the work immediately and investigate your claim.

significant contribution from periodic changes of the phase shift in PTI measurements. The relative weight of this contribution is proportional to the square root of the chopping frequency.

In conclusion the PTD method detects the elastic deformation of the medium, the MTR signal is connected only with the temperature of the surface of the material, and in the PTI technique we are dealing with a special, frequency-dependent combination of the two fields through true and apparent changes of the optical path.

¹M. A. Olmstead, N. M. Amer, S. Kohn, D. Fournier, and A. C. Boccara, *Appl. Phys. A* **32**, 141 (1983).

²J. Opsal, A. Rosencwaig, and D. L. Willenborg, *Appl. Opt.* **22**, 3169 (1983).

³A. Rosencwaig, J. Opsal, W. L. Smith, and D. L. Willenborg, *Appl. Phys. Lett.* **46**, 1013 (1985).

⁴S. Ameri, E. A. Ash, V. Neuman, and C. R. Petts, *Electron. Lett.* **17**, 337 (1981).

⁵P.-E. Nordal and S. O. Kanstad, *Infrared. Phys.* **25**, 295 (1985).

⁶G. C. Wetsel, Jr., *IEEE Transactions on Ultrasonics, Ferroelectrics and Frequency Control* **UFFC-33**, 450 (1986).

⁷A. Miklós and A. Lörincz *J. Appl. Phys.* (to be published).

⁸R. G. Stearns and G. S. Kino, *Appl. Phys. Lett.* **47**, 1048 (1985).

⁹J. Opsal and A. Rosencwaig, *Appl. Phys. Lett.* **5**, 498 (1985).

¹⁰*American Institute of Physics Handbook* (McGraw-Hill, New York, 1972).

¹¹A. Balzarotti and M. Grandolfo, *Solid State Commun* **6**, 815 (1968).

¹²W. J. Scouler, *Phys. Rev. Lett.* **18**, 445 (1967).

The axial dipole moment of two intersecting spheres of equal radii

I. W. McAllister

Physics Laboratory II, Building 309B, The Technical University of Denmark, DK-2800 Lyngby, Denmark

(Received 21 September 1987; accepted for publication 3 November 1987)

The use of a finite number of image charges to solve electrostatic problems associated with two conducting spheres intersecting at an angle of π/n (n an integer) has been known for over a century. If, however, only spheres of equal radii are considered, it is possible to extend the permissible angles of intersection to $2\pi/n$. This condition is discussed with reference to the evaluation of the axial dipole moment.

The use of a finite number of image charges to solve electrostatic problems involving conducting spheres is in general restricted to an angle of intersection α equal to π/n with n an integer. The present problem is however an exception to this condition: viz., when two intersecting spheres of equal radii are located in a uniform field E_0 oriented parallel to their axis of rotation, the electrostatic field may be deduced for $\alpha = 2\pi/n$, with $n \geq 2$ (see Fig. 1).

This situation is a direct consequence of the high degree of symmetry associated with the resultant electric field; only for spheres of equal radii is the plane containing the circle of intersection an equipotential surface, viz., the xy plane in Fig. 1. This symmetry implies that the solution for a spherical protrusion on a plane surface is also the solution to the intersecting sphere problem. For $\alpha = \pi/n$, the intersecting sphere/plane geometry represents one of the standard situations solvable with a finite number of image charges.¹ Consequently these solutions are directly applicable to two equal spheres intersecting at angles of $2\pi/n$, and, moreover, the general expressions² for the requisite systems of image charges may be used to evaluate the axial dipole moment of such intersecting spheres.

The electrostatic solution for any value of n is obtained by considering E_0 and a series of dipole/point charge images along the z axis, symmetrically positioned with respect to the xy plane. Owing to the manner in which the dipoles are located above and below the xy plane, we will refer to the upper dipoles as p_{am} and to the lower dipoles as p_{bm} . The subscript m is associated with the sequential numbering of the dipoles

and runs from 1 to m_{\max} . For $n = 2$ this situation does not arise as the solution requires only a single dipole. For n even and > 2 ,

$$m_{\max} = (n - 2)/2, \quad (1)$$

whereas for n odd we have

$$m_{\max} = (n - 1)/2. \quad (2)$$

A similar notation will be employed for the associated point charges. The magnitudes and locations of the image charges are as follows²:

$$p_{am} = p_s \left(\frac{\sin(\pi/n)}{\sin(m\pi/n)} \right)^3 = p_{bm}, \quad (3)$$

$$q_{am} = -\frac{p_s}{R} \left(\frac{\sin(\pi/n)}{\sin(m\pi/n)} \right)^2 \cos\left(\frac{m\pi}{n}\right) = -q_{bm}, \quad (4)$$

both located on the z axis at a distance h_m above/below the xy plane, where

$$h_m = R \frac{\sin(\pi/n)}{\sin(m\pi/n)} \cos\left(\frac{m\pi}{n}\right). \quad (5)$$

R is the sphere radius.

As the general solution is based on $(n - 1)$ images, then for n even a dipole is located astride the xy plane. The moment of this dipole is given by

$$p_e = p_s \sin^3(\pi/n). \quad (6)$$

p_s is the dipole moment of an isolated sphere, i.e.,

$$p_s = 4\pi\epsilon_0 R^3 E_0. \quad (7)$$

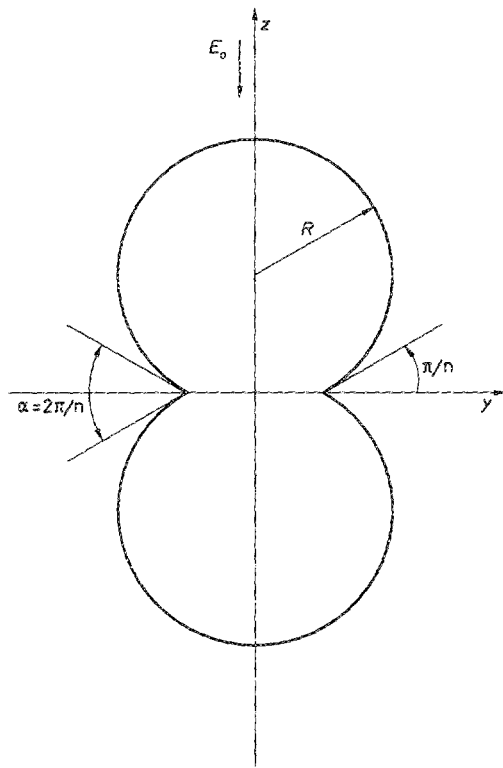


FIG. 1. Intersecting sphere geometry.

p_{am} , p_{bm} , p_e , and E_0 are all coparallel. Full details of this solution can be found in Ref. 2. To provide a fuller appreciation of specific solutions, the system of image charges for $n = 4$ and $n = 5$ are shown schematically in Fig. 2.

To evaluate the axial dipole moment p_z of the intersecting spheres, we simply sum the image dipoles and the resultant dipole of each (q_{am}, q_{bm}) pair. This leads to the following expressions:

for n odd,

$$p_z = p_{ab}, \quad (8)$$

while for n even and > 2 ,

$$p_z = p_e + p_{ab}, \quad (9)$$

where

$$p_{ab} = 2 \sum_{m=1}^{m_{\max}} (p_{bm} + h_m q_{bm}). \quad (10)$$

Upon substitution of (3)–(5) in (10), we obtain

$$p_{ab} = 2p_s \sum_{m=1}^{m_{\max}} \left(\frac{\sin(\pi/n)}{\sin(m\pi/n)} \right)^3 \left[1 + \cos^2 \left(\frac{m\pi}{n} \right) \right], \quad (11)$$

with the requisite value for m_{\max} being derived from either (1) or (2), depending upon whether n is even or odd. Finally for the trivial case of $n = 2$, we have from (6)

$$p_z = p_s. \quad (12)$$

The normalized axial dipole moment p_z/p_s for various values of n is shown in Table I. It should be noted that $n = \infty$ represents the limiting situation of two touching spheres, for which an infinite series of image charges must be considered.^{3–5} From Table I it is evident that $p_z/p_s \rightarrow 4\zeta(3)$ asymp-

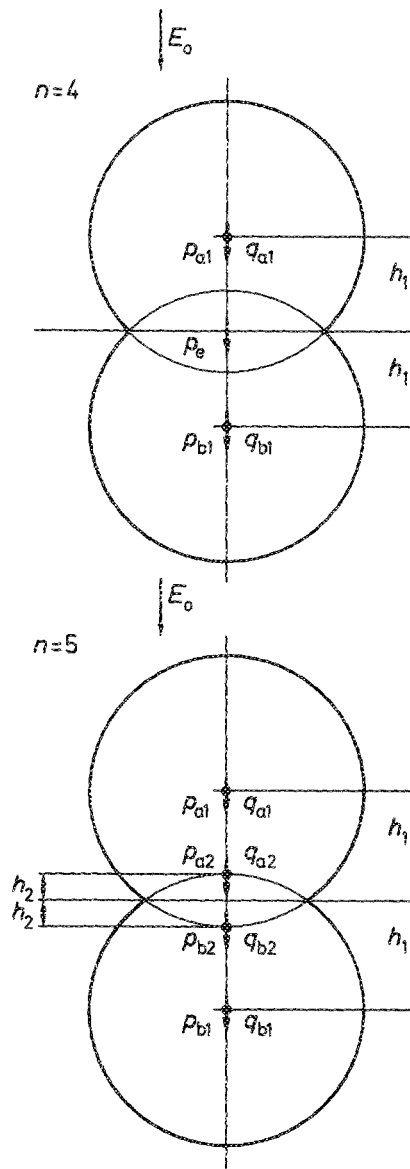


FIG. 2. Typical image solutions for n even and n odd.

TABLE I. Normalized axial dipole moment p_z/p_s of two spheres intersecting at $2\pi/n$. p_s is the dipole moment of a single sphere.

n	$2\pi/n$	p_z/p_s
2 ^a	180.0	1.0000
3	120.0	2.5000
4	90.0	3.3536
5	72.0	3.8262
6	60.0	4.1061
7	51.4	4.2832
8	45.0	4.4016
9	40.0	4.4844
10	36.0	4.5445
20	18.0	4.7411
50	7.2	4.7974
∞ ^{b,c}	0.0	4.8082

^a Represents two overlapping spheres, i.e., a single sphere.

^b From Ref. 4.

^c From Ref. 5.

totically, and hence with respect to considering variations in p_z only low n values are of interest. $\zeta(3)$ is the Riemann zeta function of argument 3, with $\zeta(3) = 1.202\,057$.⁶

In a recent publication Jones⁵ deduced the axial dipole moment for two spheres of equal radii intersecting at π/n . After using the method of inversion followed by the method of images, Jones⁵ calculates for the selected n -value the potential due to the inverse image charges, and thereafter reinverts to obtain the true potential V of the image charges with respect to the intersecting sphere geometry. Subsequently this potential is considered to represent a dipolar potential function, i.e., V is expressed in the form

$$V = (p_z/4\pi\epsilon_0 r^2) \cos \theta, \quad (13)$$

where r and θ are spherical coordinates. After some algebraic manipulation of the original V expression, an expression for the particular p_z value is obtained. In comparison the present procedure for evaluating p_z from the actual system of image charges is both general and more direct, and in addition provides solutions for angles of $2\pi/n$. In Table I, the values of p_z/p_s for $\alpha = \pi/2$ and $\alpha = \pi/3$ agree with

those published by Jones [see Eqs. (13) and (14) and Table I].⁵ With reference to the latter table, account must be taken of the constant volume constraint introduced by Jones.⁵

Further, it is worth noting that, if the uniform electric field is perpendicular to instead of parallel to the axis of rotation, the restriction to angles of π/n is upheld. Under these conditions, the solutions may be obtained utilizing $(2n - 1)$ dipole images located astride the line of centers. The transverse dipole moment p_t is thereafter obtained by summing these image dipoles, e.g., for $\alpha = \pi/2$, $p_t/p_s = 1.6464$, while for $\alpha = 0$,⁴ $p_t/p_s = 3\zeta(3)/2$. The magnitudes of these ratios illustrate the importance of p_z relative to p_t for intersecting sphere geometries.

¹J. C. Maxwell, *A Treatise on Electricity and Magnetism* (Clarendon, Oxford, 1873), Vol. I, Chap. XI.

²I. W. McAllister, *Proc. IEE A* **133**, 84 (1986).

³A. Boulloud, *C. R. Acad. Sci.* **246**, 3325 (1958).

⁴W. E. Smith and J. Rungis, *J. Phys. E* **8**, 379 (1975).

⁵T. B. Jones, *J. Appl. Phys.* **62**, 362 (1987).

⁶M. Abramowitz and I. A. Stegun, Eds., *Handbook of Mathematical Functions* (Dover, New York, 1972), Chap. 23.

Raman spectra of the pentanary alloy semiconductor

$(\text{Al}_x\text{Ga}_{1-x})_{1-z}\text{In}_z\text{P}_y\text{As}_{1-y}$

Shuichi Emura and Shun-ichi Gonda

Institute of Scientific and Industrial Research, Osaka University, Mihogaoka, Ibaraki, Osaka 567, Japan

Seiji Mukai

Electrotechnical Laboratory, Sakuramura, Niiharigun, Ibaraki 305, Japan

(Received 24 August 1987; accepted for publication 26 October 1987)

The Raman scattering of $(\text{Al}_x\text{Ga}_{1-x})_{1-z}\text{In}_z\text{P}_y\text{As}_{1-y}$ ($x < 0.33$, $y < 0.18$) pentanary alloy semiconductor lattice matched to GaAs is investigated for the first time. Five Raman peaks are found in the composition range studied here, indicating that these materials display the multimode nature in the lattice mode character. The four peaks except the lowest one in frequency are assigned to InAs-, GaAs-, GaP-, and AlAs-like longitudinal optical modes, and the lowest one to disorder activated longitudinal acoustic modes. The other possible two modes, the InP- and AlP-like modes, could not be distinguished.

The pentanary alloy semiconductor $(\text{Al}_x\text{Ga}_{1-x})_{1-z}\text{In}_z\text{P}_y\text{As}_{1-y}$ is an interesting material from the viewpoint of materials design, because in the alloy three compositional parameters can be varied independently. This type of material is usually obtained by the epitaxial growth on a substrate. In this case the number of independent compositional parameters decreases due to the lattice-matched condition. However, this material still has two independent parameters. In this material two of the various physical parameters such as the band-gap energy, refractive index, and thermal expansion coefficient can be selected independently. However, for this material, little¹ has been known about the variation of the physical parameters with parametric variation of alloy composition, in particular, lattice vibration spectrum.

In lattice vibration spectra most of the multinary alloy

semiconductors show a multimode nature. A typical example is the AlGaAs system² which indicates the two-mode behavior involving AlAs, and GaAs-like vibrations. Recent studies on the lattice vibration modes of the quaternary alloy InGaAsP on InP have given different conclusions between Raman scattering³ and infrared reflection⁴; the former persists in pseudo-two-mode behavior and the latter shows two-four-mode behavior. The Raman scattering from InGaAsP on GaAs has been reported by Inosita⁵ and displays pseudo-two-mode behavior. However, no report on nature of lattice vibration of the pentanary alloy AlGaInPAs is found up to date in literature.

In this communication, the first observation will be presented on the lattice vibration by Raman scattering in the pentanary alloy semiconductor AlGaInPAs lattice matched to GaAs. The assignment of the observed Raman bands to